MANSOURA JOURNAL OF CHEMISTRY
Official Journal of Faculty of Science, Mansoura University, Egypt
E-mail: scimag@mans.edu.eg ISSN: 2974-4938

Photothermal material based on biomass from tea waste for interfacial solar steam generation.

Raghda M. Shehata*, Mina Shawky, Awad I. Ahmed

Chemistry department, Faculty of science, Mansoura University, Egypt

**** Correspondence to:** raghdamamoud2727@gmail.com, 01270910904*

Received:19/8/2025
Accepted:12/10/2025

Abstract: Desalination is commonly used nowadays to overcome freshwater scarcity in certain parts of the world, particularly where saltwater or brackish water is available. Water treatment, desalination, and power generation all depend on the transformation of solar energy into heat to produce steam. Solar steam generation (SSG) offers a promising technique to address the global water and energy crisis with minimal environmental impact. This is achieved by using black photothermal materials, which gather solar energy and convert it into thermal energy in the form of heat. This technology relies on utilizing black nanoparticles as a light absorber, which can improve solar energy absorption and conversion efficiency. Biomass-based materials have attracted a lot of attention recently as potential ISSG substrates. This is explained by their hydrophilicity, low heat conductivity, abundance, low cost, and biocompatibility. Herein, this review explains how our evaperator biomass-based photothermal material (BC) performs for ISSG to generate clean water.

Keywords: Desalination, Interfacial evaporation, Solar energy,

1.Introduction

Water is one of the crucial elements needed for people to survive. Shortage of clean water is one of the major worldwide issues endangering humankind's survival, and needs to be solved [1]. Around the world, half a billion people are suffering from water shortages year-round, and at least once a year, four billion people experience acute water shortages [2]. Also, humans are facing an increasingly severe freshwater shortage situation as a result of the population's rapid development and the escalating issues with water pollution [3]. Even though water makes up more than 71% of the planet's surface, it can be challenging to provide freshwater to all of the demands of people, animals, and plants [4]. The World Research Institute (WRI) recently released a paper stating that approximately a quarter of the world's population faces an "extreme water shortage" crisis. Unfortunately, in addition to being scarce, freshwater resources are also inequitably distributed geographically worldwide [5].

Desalination methods for creating fresh water from seawater are receiving more attention as the world's water crisis becomes one of the biggest dangers to human society's ability to develop sustainably [6]. Recently, using solar energy has been one of the primary objectives to achieve numerous advanced desalination applications [7]. Solar-powered steam generation has gained a lot of attention lately, providing a clean water production option that uses less energy [8]. In contrast to freshwater resources, solar energy is a limitless and sustainable resource. Therefore, increasing the production of drinkable water through the use of clean and free solar energy has long been suggested as the best approach to solve the growing issue of clean water scarcity [9]. Solar-powered steam generation has gained a lot of attention lately, creating a clean water production solution that requires a lesser amount of energy [8]. Solar desalination and solar steam generation are two solar energy harvesting technologies that generate clean power and drinkable water by utilizing water resources cost-effectively. One of the most promising applications of solar energy that has attracted a lot of attention because of its numerous potential applications is solar-driven steam generation, or SSG [10]. The most effective of these solar energy usage techniques is light-to-heat conversion using a heat localizing layer that has a strong ability to absorb visible and near-infrared light, with solar thermal conversion efficiency reaching 90%[11]. Higher systematic thermal efficiency results from the interfacial solar heating system's ability to prevent heat loss to the bulk water and keep heat at the surface as compared to bulk water heating designs [6]. Because bulk water doesn't need to be heated as in traditional desalination procedures, it is a feasible green strategy that might greatly increase the efficiency of water evaporation, as the heating components can efficiently absorb solar energy and convert it into heat [12]. Various heat-localization-based solar steam generating techniques that result in effective solar-thermal conversion have been proven [13]. Theoretically, for optimal vapor generation, surface solar heating-induced vapor transpiration must coincide with surface water transportation. Enhanced light absorption, thermal insulation, mechanical strength, wettability, porosity, lifespans, and cost-effectiveness are also necessary for a successful photo-thermal conversion evaporator[14]. Carbon materials, semiconductors, and plasmonic metals are among the many types of photothermal materials (absorbers) that are frequently employed to capture solar energy and accomplish effective photothermal conversion [15]. Besides plasmonic nanoparticles, graphene oxide (GO), reduced GO (RGO), and single-walled carbon nanotubes are examples of nanostructured carbon-based materials that have recently been used in photothermal energy conversion. Because of their exceptional photothermal transduction capabilities, which enable them to capture visible and near-infrared (NIR) light portions of the electromagnetic spectrum and transform the absorbed radiation into heat through nonradiative decay processes [16].

Carbon-based materials usually possess better chemical stability and are less expensive than metallic nanomaterials and black semiconductors, as well as endure environments that are alkaline, salty, and acidic [17].

The International Tea Committee's study states that over 5.8 million tons of tea were consumed worldwide in 2019 [18]. Specifically, 78% of the tea consumed globally is black tea, which generates a lot of trash during the brewing process [19]. Even though black tea waste can be used as a biomass source and is known as biochar (BC), a significant amount of it is typically thrown away. When biomass—such as sawdust, grass, and wheat straw—is heated to 350–700 degrees Celsius in an inert environment, a carbon-rich substance known as BC is created [20]. Furthermore, BC is inexpensive, reusable, and has good light-to-heat conversion qualities, making it a common material in our daily lives [21].

Herein, tea waste was used as a precursor to create porous biochar in a simple, inexpensive, and scalable method. In addition to having numerous holes that could provide broad channels for water circulation, the generated BC had a suitable specific surface area that could absorb all of the solar energy. According to the obtained results, to achieve outstanding results in solar-powered evaporation, fabricated membranes were characterized by open porosity for capillarity, low thermal conductivity, and great solar absorption. Furthermore, the BC's high desalination capacity, consistency, affordability, and ease of preparation make it a viable option for sustainable saltwater desalination

2. Materials and procedures

2.1. Chemicals and materials

The chemicals used in this investigation were all purchased commercially and did not undergo any further purification. The tea waste, collected after using it, was used as the precursor for the biomass-derived BC. Hydrochloric acid (HCl, 1N), Sodium alginate (SA), Calcium chloride ($CaCl_2$), and absolute ethanol were purchased from Sigma-Aldrich. Distilled water obtained from the Millipore water system was used to prepare all aqueous solutions.

2.2. Synthesis of biochar (BC)

After collecting the tea waste, it was continuously cleaned with deionized water to remove dust, and then boiled until it turned a light yellow to eliminate any dissolved residue. Following that, the tea was filtered out of the solution and dried for 48 hours at 80 °C in a conventional oven. After the dried tea was finely powdered, it was thermally treated at 700 °C under a nitrogen gas flow (150 mL/min) for 2 h. The produced powder was treated with HCl (1.0 M) for 24 hours to get rid of any last bits of residue. The resulting carbon was further separated using a centrifuge and repeatedly cleaned with deionized water till pH 7 before being dried overnight at 80 °C. Then, after being ground into a fine powder, the finished BC product was run through a 0.16 mm sieve.

2.3. Synthesis of photothermal absorber

The usual procedure was to disperse 0.5 g BC in 20 mL of deionized water, sonicate it for 1 hour, then add 0.04 g of sodium alginate to the mixture, suspend it for 30 minutes, followed by stirring for another 30 min. After that, a cotton pad was painted with the black suspension using a painting brush and was utilized as the upper layer's solar absorber. Next, 0.3 g of $CaCl_2$ dissolved in 25 ml solution was added as a crosslinker, drop-wise under gentle heat until the formation of a gelatinous layer. To produce a uniform coating of photothermal absorber, the black-formed disk had been dried at 80 °C overnight**.**

2.4. Material Characterization

Several techniques of analysis were employed to demonstrate the as-prepared samples' adequate preparation. To investigate the functional groups in the structure, FT-IR patterns were carried out using a MATTSON IR-5000S spectrophotometer equipped with a diamond-attenuated total reflectance (FT-DATR in wavenumber ranging from 4000 to 500 cm^{-1}). Utilizing scanning electron microscopy (SEM, JEOL JSM 6510 lv), an investigation was carried out to examine the materials' surface structure and elemental composition. The constructed evaporators were exposed to radiation from a solar simulator (SciSun-300 AAA) with a 300 W xenon light source and an AM 1.5G filter in order to evaluate the SSG performance. The evaporators' surface temperatures were simultaneously estimated using an infrared thermal camera (IR-camera, httixintai), which were also recorded as a function of time using a thermocouple, and TES-1333R, a digital sunlight meter, for measuring light intensity.

2.5. Interfacial solar steam generation (ISSG) experiments

The system used in the ISSG is a bilayer system consisting of an upper layer (photothermal absorber, Black material BC and a bottom layer (an insulator, polyethylene (PE)). To keep the material from coming into contact with the water, the PE insulator is positioned between the water and the photothermal conversion layer. Rather than heating the bulk water at the bottom, the thermal insulating foam ensures that heat loss may be minimized and that water evaporation uses as much thermal energy as possible [22]. A disk of commercial PE foam was drilled, and 8 cotton wicks penetrated the PE disk; then, Water can be transferred to the thermal interface in a continuous flow by cotton because of the capillary phenomena. Also, cotton is thought to be a promising predecessor of ISSG because of its strong hydrophilicity, low heat conductivity, and good stability [23]. The prepared system was floated above 250 mL of salt water or distilled water, after the photothermal absorber layer was placed on top of the bottom layer. The ISSG device's simulation of sun irradiation was used to assess the steam generation efficiency. By utilizing a 300 W xenon arc lamp throughout a 1 kW m^{-2} (1 sun) solar simulator, sunlight was simulated. Every practical experiment was carried out at room tempreture and a 60% relative humidity. The light intensity was measured with an optical power meter before each experiment. In order to eliminate heat loss to bulk water, the absorption layer floats on the water, and the photothermal disk is placed in the center of a 250 mL glass beaker. Following exposure to a solar simulator, the ISSG system's prepared photothermal membrane absorbs solar energy and transforms it into thermal energy, and a fiber cotton wick is used to transport the bulk water.

To measure the mass loss of water, an electronic analytical balance was utilized at a particular time every five minutes for 60 minutes of sunlight. To illustrate the temperature change on the foams' surface before and after sun irradiation, an infrared camera was utilized. The experiment used saltwater simulation (3.5, 10, and 20 weight percent salt, 250 mL) and was left in the dark for 30 minutes to attempt adsorption saturation to measure efficiency when it comes to salty water.

2.6. Photothermal conversion efficiency and steam generation rate

Equation (1) was used to evaluate the ISSG System's evaporation rate (kg m^{-2} h^{-1}) derived from solar.

$$v = \frac{dm}{S\,dt} \qquad (1)$$

where t (h) is the evaporation time, S (m2) is the illuminated area of the artificial photothermal disk, and the difference in water weight between the dark and solar irradiation phases is expressed in dm (kg). A photothermal conversion efficiency (η) under 0.5, 1, 2, and 5 sun irradiation can thus be calculated as follows (1 sun = 1 kW m^{-2}):

$$\eta = \frac{H_e v}{Q_{in}} \qquad (2)$$

where Qin is a measure of the solar radiation's power density (1000 W m^{-2}) and v (kg m^{-2} h^{-1}) represents the evaporation flow of water under solar irradiation. The following formula can be used to measure the evaporation enthalpy of water at the surface temperature of the evaporators that induce the evaporation:

$$He = C\Delta T + \Delta h \qquad (3)$$

where ΔT (K) is the temperature differential between the bulk water and the evaporator surface. The standard enthalpy (Δ*h*) of water vaporization (2394 kJ kg^{-1}), and C is the specific heat capacity of water (4.18 j g^{-1} k^{-1}).

3. Results and Discussion

3.1. Specifications of the Material

The presence of organic functional groups in the BC was indicated by the FTIR spectrum.

As shown in Fig. 1, the loss of labile aliphatic molecules was indicated by the strong O-H stretching band from 3217 to 3650 cm^{-1} and a very weak C-H stretching band at 2954 cm^{-1} [24]. Peaks around 1822 to 2322 cm^{-1} indicated the carboxylic bond, whereas the C=O stretching of aromatic rings was demonstrated by the spectra at 1500 and 1570 cm^{-1} [25].

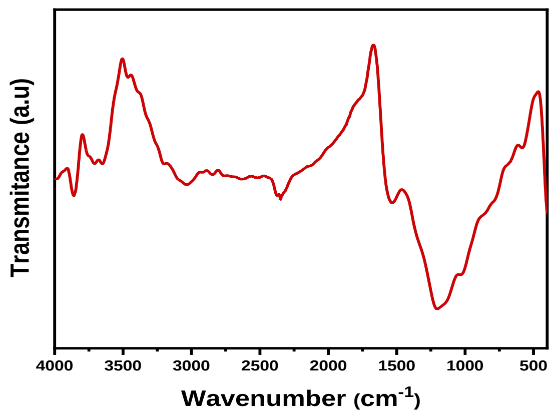

Fig.1 FT-IR spectrum of BC.

The morphologies in Figure (2) were examined using SEM analysis. SEM pictures demonstrate that BC has a very well-developed, porous surface [26].

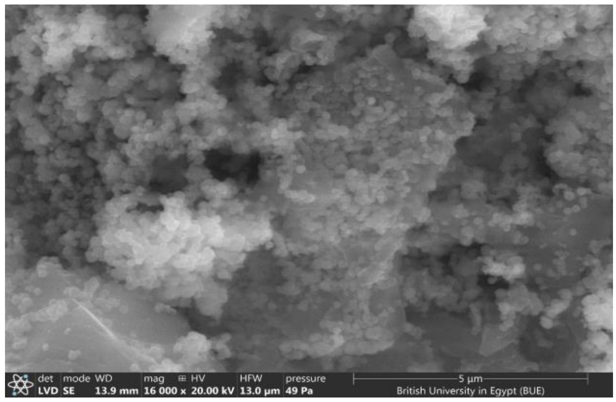

Fig. 2. SEM images of BC.

3.2. Interfacial solar steam generation Results

There are two distinct layers that make up the bilayer photoabsorber system: a black membrane based on BC (Top layer) and a thick insulating foam layer (PE, bottom layer). The black photothermal material was simply applied onto the surface of the cotton pad and assembled to make an efficient solar steam generator. The insulating foam ensures little heat loss to the evaporator's bulk water and provides buoyancy to the bilayer architecture. Because of the very hydrophilic nature of cellulose and the capillary nature enforced through these macrochannels, the cellulose skeleton of cotton fabric is made up of anisotropic, vertically extending macrochannels that function as water channels to move water upward. Nine cotton wicks were evenly spaced on the foam disk to allow the water to be readily pumped up through the insulator. Furthermore, thermal control is essential to the ISSG system's efficient operation. The ideal situation is that all of the heat produced is utilized to evaporate the water on the solar absorber's surface, which is usually connected to a pore-filled, water-like, floating support. Cotton pad and BC samples were used to make two systems with a 5.0 cm diameter in order to evaluate the performance of steam generation for different manufactured photothermal absorbers.

The mass loss of pure water, Cotton pad, and BC photoabsorber systems was 0.3, 0.72, and 1.33 kg m^{-2}, respectively during one hour of exposure to sunlight, as shown in Fig. 3a. The mass loss of the Fabricated materials when there is 3.5% salts under one sun's illiumination is shown in Fig. 3b; BC showed the greatest mass loss under one sun's illumination.

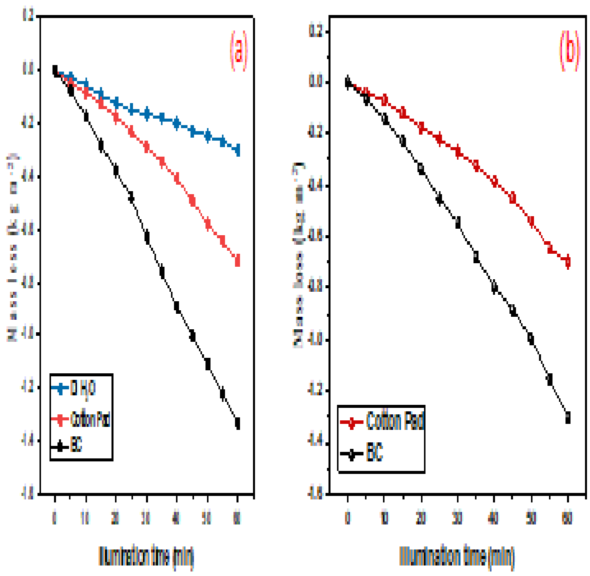

Fig. 3. Mass loss curves when (a) tape water and (b) simulated saline water are present.

Therefore, using high-quality photothermal materials is essential. Also, creating sensible structure designs in order to generate solar steam effectively. According to the evaporation efficiency graph in Fig. 4a, BC obtained a steam efficiency of 88.7%.

The estimated BC photothermal efficiency when saline water with varying salt concentrations is present are shown in Fig. 4b. The observed efficiency at varying salt concentrations were 88.7% for tap water and 86.8%, 85.9%, and 84.8% for 3.5, 10%, and 20%, respectively. Therefore, a good impact of salt rejection was demonstrated by the manufactured ISSG system.

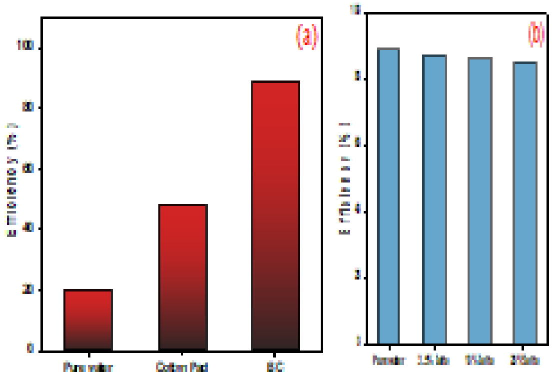

Fig. 5. Evaporation efficiencies of fabricates samples, and (b) Efficiencies of BC in the presence of saline water with different salt concentrations.

The evaporation system's capacity to produce steam is significantly impacted by the quantity and intensity of light. To assess the photothermal's stability, our system's ISSG performance is examined under various solar irradiation conditions, as plotted in Fig.5. After one hour of exposure to intense light from one, two, and five suns, the BC photothermal system's evaporator demonstrated good mass loss values of 1.33, 2.66, and 6.65 kg m^{-2}, respectively.

That indicates BC is regarded as a potential option for sustainable seawater desalination.

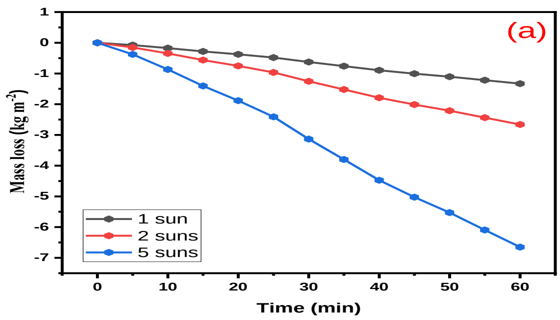

Fig.6. (a) Mass loss plot of BC under a different number of suns

4. Conclusion

One of the major worldwide issues that threatens the continuity of humankind and needs is the scarcity of clean water, which must be solved immediately. A perfect way to overcome the shortage of freshwater resources is to use solar energy to generate steam.

In this study, based on BC, a tea waste biomass is used as a photothermal material for solar steam generation. The BC photothermal system demonstrated an outstanding evaporation rate

of 1.4 kg m^{-2} h^{-1} with a conversion efficiency of 95.7% when exposed to one sun's light. The manufactured system also showed excellent salt rejection, high desalination efficiency, and long-term dependability. The produced device will be a potential solar conversion material in desalination because of BC's easy production, low cost, non-toxicity, strong reusability, and high efficiency.

4. References

1. Sharshir, S. W.; Algazzar, A. M.; Elmaadawy, K. A.; Kandeal, A. W.; Elkadeem, M. R.; Arunkumar, T.; Zang, J.; Yang, N., (2020) New hydrogel materials for improving solar water evaporation, desalination and wastewater treatment: A review. Desalination**,** 491.
2. Xu, J.; Wang, Z.; Chang, C.; Fu, B.; Tao, P.; Song, C.; Shang, W.; Deng, T., (2020) Solar-driven interfacial desalination for simultaneous freshwater and salt generation. Desalination**,** 484.
3. Huang, Q.; Liang, X.; Yan, C.; Liu, Y., (2021) Review of interface solar-driven steam generation systems: High-efficiency strategies, applications and challenges. Applied Energy**,** 283.
4. Alkaisi, A.; Mossad, R.; Sharifian-Barforoush, A., (2017) A Review of the Water Desalination Systems Integrated with Renewable Energy. Energy Procedia**, 110**, 268-274.
5. Shatat, M.; Worall, M.; Riffat, S., (2013) Opportunities for solar water desalination worldwide: Review. Sustainable Cities and Society**, 9**, 67-80.
6. Liu, H.; Huang, Z.; Liu, K.; Hu, X.; Zhou, J., (2019) Interfacial Solar-to-Heat Conversion for Desalination. Advanced Energy Materials**, 9 (21)**.
7. Arunkumar, T.; Wang, J. Denkenberger, D., (2021) Capillary flow-driven efficient nanomaterials for seawater desalination: Review of classifications, challenges, and future perspectives. Renewable and Sustainable Energy Reviews**,** 138.
8. Fang, Q.; Li, T.; Chen, Z.; Lin, H.; Wang, P.; Liu, F., *(*2019) Full Biomass-Derived Solar Stills for Robust and Stable Evaporation To Collect Clean Water from Various Water-Bearing Media. ACS Appl Mater Interfaces**, 11 (11)**, 10672-10679.
9. Storer, D. P.; Phelps, J. L.; Wu, X.; Owens, G.; Khan, N. I.; Xu, H., (2020) Graphene and Rice-Straw-Fiber-Based 3D Photothermal Aerogels for Highly Efficient Solar Evaporation. ACS Appl Mater Interfaces**, 12 (13)**, 15279-15287.
10. Dao, V. D.; Choi, H. S., (2018) Carbon-Based Sunlight Absorbers in Solar-Driven Steam Generation Devices. Glob Chall**, 2** (**2**), 1700094.
11. Jiang, F.; Liu, H.; Li, Y.; Kuang, Y.; Xu, X.; Chen, C.; Huang, H.; Jia, C.; Zhao, X.; Hitz, E.; Zhou, Y.; Yang, R.; Cui, L.; Hu, L., (2018) Lightweight, Mesoporous, and Highly Absorptive All-Nanofiber Aerogel for Efficient Solar Steam Generation. ACS Appl Mater Interfaces**, 10 (1)**, 1104-1112.
12. Chen, R.; Zhu, K.; Gan, Q.; Yu, Y.; Zhang, T.; Liu, X.; Ye, M.; Yin, Y., (2017) Interfacial solar heating by self-assembled Fe3O4@C film for steam generation. Materials Chemistry Frontiers**, 1 (12)**, 2620-2626.
13. Behera, S.; Kim, C.; Kim, K., Solar (2020) Steam Generation and Desalination Using Ultra-Broadband Absorption in Plasmonic Alumina Nanowire Haze Structure-Graphene Oxide-Gold Nanoparticle Composite. Langmuir**, 36** (**42**), 12494-12503.
14. He, J.; Zhang, Z.; Xiao, C.; Liu, F.; Sun, H.; Zhu, Z.; Liang, W.; Li, A., (2020) High-Performance Salt-Rejecting and Cost-Effective Superhydrophilic Porous Monolithic Polymer Foam for Solar Steam Generation. ACS Appl Mater Interfaces**, 12 (14)**, 16308-16318.
15. Zang, L.; Finnerty, C.; Zheng, S.; Conway, K.; Sun, L.; Ma, J.; Mi, B., (2021) Interfacial solar vapor generation for desalination and brine treatment: Evaluating current strategies of solving scaling. Water Res**, 198**, 117135.
16. Awad, F. S.; Kiriarachchi, H. D.; AbouZeid, K. M.; Özgür, Ü.; El-Shall, M. S., (2018) Plasmonic Graphene Polyurethane Nanocomposites for

Efficient Solar Water Desalination. ACS Applied Energy Materials**, 1 (3)**, 976-985.
17. Li, G.; Law, W.-C.; Chan, K. C., (2018) Floating, highly efficient, and scalable graphene membranes for seawater desalination using solar energy. Green Chemistry**, 20 (16)**, 3689-3695.
18. Guo, S.; Kumar Awasthi, M.; Wang, Y.; Xu, P., (2021) Current understanding in conversion and application of tea waste biomass: A review. Bioresour Technol**, 338**, 125530.
19. Eom, H.; Kim, J.; Nam, I.; Bae, S., (2021) Recycling Black Tea Waste Biomass as Activated Porous Carbon for Long Life Cycle Supercapacitor Electrodes. Materials (Basel)**, 14 (21)**.
20. Akgül, G.; Iglesias, D.; Ocon, P.; Moreno Jiménez, E., (2019) Valorization of Tea-Waste Biochar for Energy Storage. BioEnergy Research**, 12 (4)**, 1012-1020.
21. Shi, L.; Wang, Y.; Zhang, L.; Wang, P., (2017) Rational design of a bi-layered reduced graphene oxide film on polystyrene foam for solar-driven interfacial water evaporation. *Journal of Materials Chemistry A***, 5 (31)**, 16212-16219.
22. Lin, Y.; Zhou, W.; Di, Y.; Zhang, X.; Yang, L.; Gan, Z., (2019) Low-cost carbonized kelp for highly efficient solar steam generation. AIP Advances**, 9 (5).**
23. Bai, Z.; Xu, H.; Yang, B.; Yao, J.; Li, G.; Guo, K.; Wang, N.; Liang, N., (2022) Fe(3)O(4)/Diatomite-Decorated Cotton Evaporator for Continuous Solar Steam Generation and Water Treatment. Materials (Basel)**, 15 (17)**.
24. Divya Pal a; b, S. K. M., (2018) Abatement of cadmium (Cd) contamination in sediment using tea waste biochar through meso-microcosm study. *Journal of Cleaner Production*.
25. Cao, X.; Harris, W., (2010) Properties of dairy-manure-derived biochar pertinent to its potential use in remediation. Bioresour Technol**, 101 (14)**, 5222-8.
26. Keerthanan, S.; Bhatnagar, A.; Mahatantila, K.; Jayasinghe, C.; Ok, Y. S.; Vithanage, M., (2020) Engineered tea-waste biochar for the removal of caffeine, a model compound in pharmaceuticals and personal care products (PPCPs), from aqueous media. Environmental Technology & Innovation**,** 19.